Ambient Vibration Study of the Gi-Lu Cable-Stay Bridge: Application of Wireless Sensing Units

Kung-Chun Lu[1], Yang Wang[2], J. P. Lynch[3], C. H. Loh[1]
Yen-Jiun Chen[1], P. Y. Lin[4], Z. K. Lee[4]

[1] Department of Civil Engineering, National Taiwan University, Taipei, Taiwan
[2] Dept. of Civil & Environmental Engineering, Stanford University, Stanford, USA
[3] Dept. of Civil & Environmental Engineering, University of Michigan, Ann Arbor, USA
[4] National Center for Research on Earthquake Engineering, Taipei, Taiwan

ABSTRACT

An extensive program of full-scale ambient vibration testing has been conducted to measure the dynamic response of a 240 meter cable-stayed bridge – Gi-Lu Bridge in Nan-Tou County, Taiwan. A MEMS-based wireless sensor system and a traditional microcomputer-based system were used to collect and analyze ambient vibration data. A total of four bridge modal frequencies and associated mode shapes were identified for cables and the deck structure within the frequency range of 0~2Hz. The experimental data clearly indicated the occurrence of many closely spaced modal frequencies. Most of the deck modes were found to be associated with the cable modes, implying a considerable interaction between the deck and cables. The results of the ambient vibration survey were compared to modal frequencies and mode shapes computed using three-dimensional finite element modeling of the bridge. For most modes, the analytical and the experimental modal frequencies and mode shapes compare quite well. Based on the findings of this study, a linear elastic finite element model for deck structures and beam element with P-Delta effect for the cables appear to be capable of capturing much of the complex dynamic behavior of the bridge with good accuracy.

Keywords: Input unknown identification, Stochastic system identification, Ambient vibration, Wireless sensors

1. INTRODUCTION

One of the engineering challenges of cable-supported bridges is in understanding and allowing for the dynamic response to effects of traffic, wind and earthquakes. Investigation of both aerodynamic stability and earthquake response of cable-stayed bridges are dependent on the knowledge of the structure's dynamic characteristics, such as modal frequencies, mode shapes and modal damping values, as well as a description of the dynamic loading. Conducting full-scale dynamic tests is one of the most reliable ways of assessing the actual dynamic properties of these structures. Such tests serve to complement and enhance the development of analytical techniques and models that may be applied to dynamic analysis. During the past two decades, many researchers have conducted full-scale dynamic tests on suspension bridges, however, there is less information available on full-scale dynamic testing of cable-stayed bridges. Some typical examples of full-scale dynamic tests on bridges are provided in the references [1~4].

A simpler method for the determination of dynamic characteristics of structures is through ambient vibration measurements. The ambient vibration behavior of a structure is recorded, evaluated and interpreted under ambient influence, i.e. without artificial excitation, by means of highly sensitive velocity or acceleration sensors. The rapid development of measuring technology, on the one hand, and computer technology including software, on the other, enables us to carry out dynamic measurement of ambient structural vibrations and evaluation quickly. The dynamic characteristics which were extracted from the vibration signals are not only used for a single check of calculation models, but also for statements on the chronological development of the load-bearing capacity.

The use of wireless communication for structural health monitoring (SHM) data acquisition was illustrated by Straser and Kiremidjian [5]. Recently, Lynch *et al.* extended the work by embedding damage identification algorithm into wireless sensing units [6, 7]. With the rapid advancement of sensing, microprocessor, and wireless technologies, it is possible to assess the benefits from the application of such technologies in the structural engineering field. The

purpose of this paper is to use the developed wireless modular monitoring system (WiMMS)[8] for civil infrastructural health monitoring. Towards this end, this study will determine experimentally the dynamic properties of the newly retrofitted Gi-Lu cable- stayed bridge using ambient vibration signals. A newly developed ambient vibration system which incorporated the wireless modular monitoring system was implemented in this full-scale experiment. A stochastic system identification method was used to identify the dynamic properties of the bridge. Finally, the comparison between the numerical modeling results and the experimental results is discussed.

2. AMBIENT VIBRATION MEASUREMENTS

The cable-stayed bridge used for this study is the Gi-Lu bridge, located at Nantou County, Taiwan. It is a modern designed pre-stressed concrete cable-stayed bridge, which crosses the Juosheui River in Taiwan. The bridge has a single pylon (58 meters height above the deck), two rows of harped cables (68 cables in total). With 2.75 meters in depth and 24 meters in width, the box girder rigidly connects with the pylon and spans 120 meters to each side span.

2.1 Instrumentation and data acquisition

The instrumentation system consisted of the following components:

Transducers: 9 Tokyo Sokushin VSE-15 velocity detectors with sensitivity factors of 0.25Volt/1 kine.
Wireless sensing unit: 9 wireless sensing units, each with voltage converters and power supply systems.
Microcomputer: one PC microcomputer with wireless modem to serve as the trigger and recoding system.

Three test procedures were conducted. First, the vertical dynamic response of the bridge deck was measured by 9 transducers placed at various location (from the Gi-Gi side of the bridge, each sensor was placed 30 meters apart). Data were sampled 100 points per second per channel to provide good waveform definition. The digital signals were transmitted by the wireless sensing units to a central PC microcomputer serving as the monitoring system's data repository. Fig. 1 shows the location of the sensors. Second, both cable and deck vibrations were measured simultaneously. The sensors on the cable will be shown in Fig. 7. Finally, calibration of all the sensors was conducted by first placing them all in the same location to check the consistency of the vibration amplitude in all frequencies.

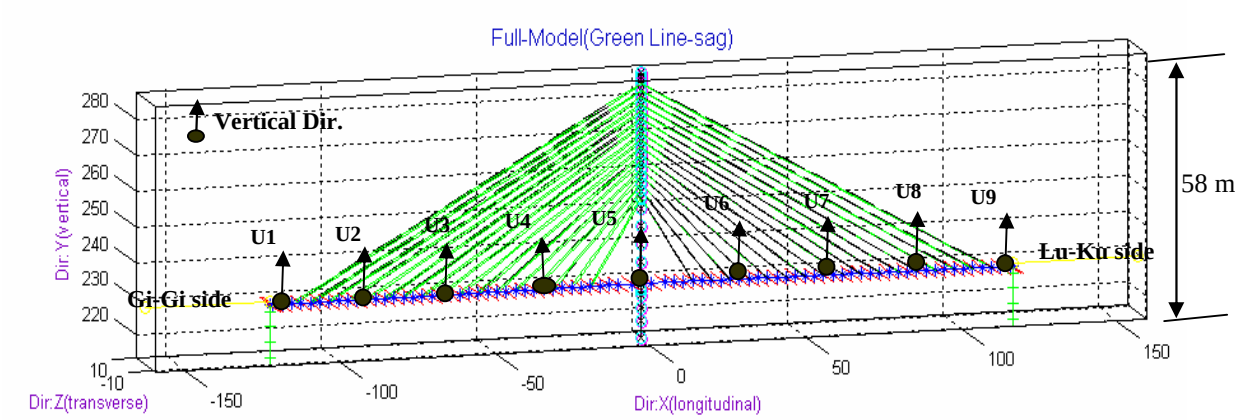

Fig. 1: Ambient vibration test configuration for vertical measurement,

2.2 Wireless sensor for vibration measurement

Since wireless sensing units were used in this test which replaced the traditional data acquisition system that uses cables, the wireless sensing unit developed by Lynch was introduced [8]. The wireless sensing unit includes three subsystems: the sensing interface, the computation core, and the wireless communication system. The sensing interface is responsible for converting the analog sensor signals into digital forms. The digital data is then transferred to the computational core by the a serial peripheral interface (SPI) port. External memory is associated with the computational core for local data storage or analysis. The hardware profile and functional design of wireless modular monitoring system is shown in Fig.2. The Maxstream XStream wireless modem, operating on 2.4 GHz, is used for the wireless communication subsystem. Its outdoor communication range is up to 300m line-of-sight.

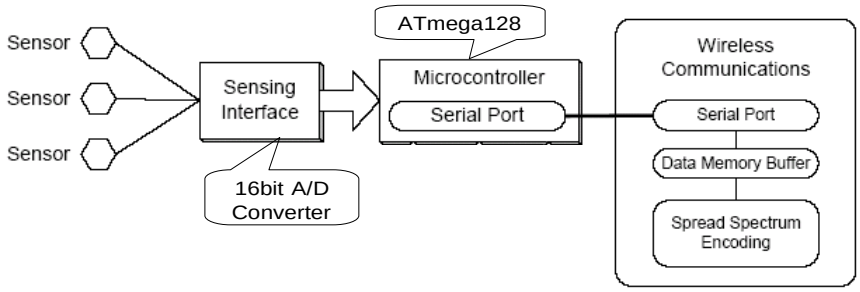

Fig. 2: Hardware functional diagram of the wireless sensing unit.

To implement the wireless sensor for ambient vibration measurement, a signal converter needs to be developed. The wireless sensing unit was designed to accept any analog signal output ranging between 0 and 5 Volt; however, sensors with outputs falling outside of this range can not be directly employed thereby constraining the wireless modular monitoring system. For example, the Tokyo Sokushin VSE-15 velocity detector was used to measure the ambient vibration signal in this study. The maximum output signal from the velocity sensor was ±10 volt which can not meet the input requirement of wireless sensing unit (0~5V). A signal converter must therefore be designed. Fig. 3 shows the arrangement of the voltage converter designed for this study.

For ambient vibration survey of the bridge, a total of 12 sensing units were used simultaneously. Fig. 4 shows the calibration setup of the wireless sensors (all placed in the same location) on the bridge deck. A directional antenna (D-link) was used to enhance the signal communication and to extend the range of the sensors in the field.

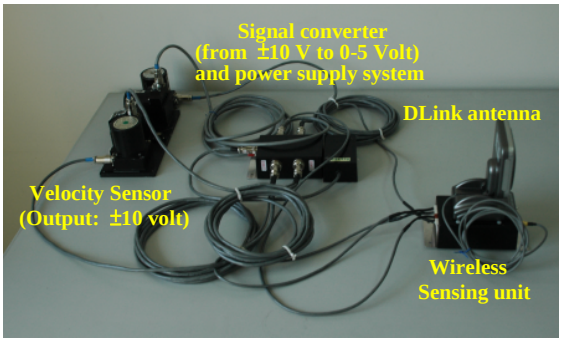

Fig.3: A signal converter between the velocity meter and the wireless sensing unit.

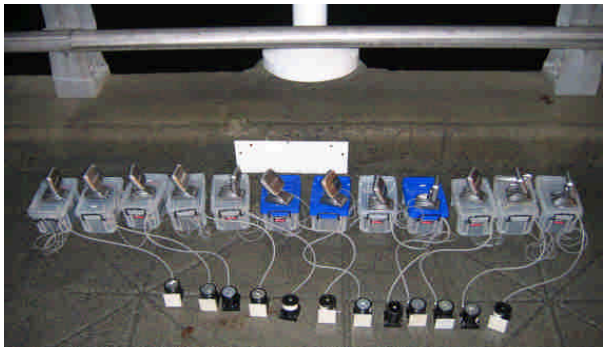

Fig. 4: Calibration layout of sensors at the bridge deck. The sensing unit, converter and power supply system are covered by plastic box .

2.3 Analysis of structural ambient vibration data

There are several methods of data analysis which have been used for system identification using recorded ambient vibrations. In this study two different approaches are used to identify the dynamic characteristics of the vibration structure. First, the model estimation through correlation function is introduced. The method of transfer function poles, which is basically a discrete time technique, will be used in this method. Based on the classical normal modes approach, any response quantity *y(t)* of a linear MDOF system is linearly related to the normal coordinate

$$y(t) = \sum_{m=1}^{M} B_m y_m(t) \tag{1}$$

The z-domain representation of the transfer function, H(z), is represented as follows:

$$H(z) = \frac{A(z^{-1})}{\prod_{m=1}^{M}(1-\varphi_{1m}z^{-1}-\varphi_{2m}z^{-2})} = \frac{Y(z)}{X(z)} \tag{2}$$

In the above equation $A(z^{-1})$ is a polynomial of order *2M-1,*and the denominator is a order of *2M*. The input-output difference equation can be obtained by taking the inverse z-transform of both side of Equation **2** to get

$$\begin{aligned} y(n)-\varphi_1 y(n-1)-\cdots-\varphi_{2M} y(n-2M) = \\ \alpha_1 x(n-1)+\alpha_2 x(n-2)+\cdots+\alpha_{2M-1} x(n-2M+1)=0 \end{aligned} \tag{3}$$

Multiplying both sides of this equation by *y(n-k)* and taking expectations for k>2M we have

$$R_y(k)-\varphi_1 R_y(k-1)-\cdots-\varphi_{2M} R_y(k-2M)=0 \tag{4}$$

which is the difference equation of the response autocorrelation function given that the forcing function is a white noise process. For ambient vibration survey, this is a correct assumption. The estimated autocorrelation function is defined as:

$$\hat{R}_y(k) = 1/N \sum_{n=k}^{N} y(n)y(n-k) \tag{5}$$

A least squares estimate of the coefficient vector $\hat{\Phi}$ becomes

$$\hat{\Phi} = (X^T X)^{-1} X^T Y \tag{6}$$

where $$\hat{\Phi}^T = [\varphi_1, \varphi_2, \cdots, \varphi_{2M}] \quad and \quad Y^T\left[\hat{R}_y(2M), \hat{R}_y(2M+1), \cdots, \hat{R}_y(K_{\max}\right] \tag{6a}$$

and

$$X = \begin{bmatrix} \hat{R}_y(2M-1) & \hat{R}_y(2M-2) & . & \hat{R}_y(0) \\ \hat{R}_y(2M) & \hat{R}_y(2M-1) & . & \hat{R}_y(1) \\ . & . & . & . \\ \hat{R}_y(K_{\max}-1) & \hat{R}_y(K_{\max}-2) & . & \hat{R}_y(k_{\max}-2M) \end{bmatrix} \tag{6b}$$

By taking z-transform of the correlation equation, the complex roots of the characteristics equation will provide necessary information for the estimation of the modal frequencies and damping. Since all the coefficients of the characteristics equation are real, the roots will appear as complex conjugate pairs corresponding to on of the M observed modes. The denominator of equation can be expressed as a summation of M-modes [9]:

$$\sum_{k=1}^{M}\left[1-2p_k^R z^{-1}+|p_k|^2 z^{-2}\right] \tag{7}$$

where p_k is the k-th root of the characteristic equation and *R* denotes the real part of the root. The calculated modal frequencies and damping ratios in terms of the poles of the discrete system as:

$$\xi_k = \ln(1/|p_k|)/\left[\upsilon_k + \ln(1/|p_k|) \quad and \quad f_k = \ln(1/|p_k|)/2\pi\xi_k\Delta\right] \tag{8}$$

Where υ_k =the augment of p_k $\left[i.e.\ \tan(\upsilon_k) = (p_k^i / p_k^R)\right]$. The frequencies and damping ratios corresponding to a complex pair of $p_k's$ are identical. Therefore, the above equation leads to only different ξ_k and f_k values.

2.4 Stochastic subspace identification

The stochastic subspace identification method (SSI), as presented by Van Overschee and De Moor [10], is a method to identify the stochastic state space model from output-only measurement by using robust numerical techniques such as QR-factorization, singular value decomposition (SVD) and least squares. The QR-factorization results in a significant data reduction, where as the SVD is used to reject system noise. Once the mathematical description (the state space model) of the structure is found, it is straightforward to determine the modal parameters (by an eigenvalue decomposition): natural frequencies and mode shapes. The first step to conducting the method is to gather the output measurement to form the Hankel matrix with *2i* block rows and *j* columns. The Hankel matrix can be divided into a past reference and a future part:

$$H = \begin{pmatrix} Y_{0,i-1}^{ref} \\ \hline Y_{i,2i-1} \end{pmatrix} = \begin{pmatrix} Y_p^{ref} \\ \hline Y_f \end{pmatrix} \begin{matrix} \updownarrow ri \ "past" \\ \updownarrow li \ "future" \end{matrix} \tag{9}$$

In this experiment the first *i* block (Y_p^{ref}) is set to 5 rows and 1000 columns (which is equal to 10 second of record) and data from Channel U3 was selected as the reference. The rest of the data from different channels is put into Y_f. For

each channel, the data is constructed with dimension of (5 x 1000). A total of 8 channels of response data are used to form the lower part of the Hankel matrix. Take the QR-factorisation of the block Hankel matrix ($H=RQ^T$), then the projection of the row space of the future outputs into the row space of the past reference output can be evaluated. The main theorem of stochastic subspace identification states that the projection can be factorized as the product of the observability matrix and the Kalman filter state sequence. This is the reference-based data driven stochastic subspace identification.

3 DYNAMIC PROPERTIES OF THE DECK AND CABLES

3.1 Results from analytical finite element model [11]

Before the identification of dynamic properties of the bridge from ambient vibration data the analytical result of the bridge was described. In the analytical model, the finite element model of the cable-stayed bridge has a total of 1,009 nodes. The pylon is modeled by 90 nodes with 540 degrees-of-freedom (DOFs) (25 nodes are above the deck, 5 nodes are below the deck, and 60 nodes are near the anchors). The deck is modeled by 729 nodes with 4,374 DOFs. Pier2 (under the pylon) is modeled by 5 nodes (including the node attached to the ground). Pier1 (North side) and pier 3 (South side) have 4 nodes for each (including the node attached to the ground) with a total of 56 DOFs. The cable is modeled with 9 nodes for each cable and total of 612 nodes for 64 cables with 3,672 DOFs. The mass matrix is formed by a lumped mass approach. The proportional damping formulation is used in each element and then to form the full damping matrix is formed with the same procedure as is used to form the stiffness matrix. The damping ratio for deck, pylon and piers (including all supports) is assumed to be 5% and for cables is assumed to be 1%. Constraints are applied to restrain both ends of the deck (boundary conditions). All DOFs at the bottom of both piers are fixed. As for the boundary condition of the bridge structure, all translational DOFs and torsion DOF at the side spans connected to the embankment are fixed. The transverse and vertical degrees of freedom at piers 1 and 3, and at the side spans of the bridge deck, deform consistently (i.e. y- and z- directions are constraint, and x-,φ_x -, φ_y -, φ_z – directions are free to move.). For modeling the cable, the geometric nonlinear beam element was generated which included the nonlinear term plus the conventional linear beam element. The estimated five dominant vibration frequencies of the deck is shown in Table 1 and the corresponding mode shapes will be shown later. The estimated vibration frequencies of cables (shortest cable R1, middle length cable R17, longest cable R33) are shown in Table 2. From the results of the analytical finite element model, it is found that the second deck vibration mode corresponds to the 31-th mode in the finite element model. The modes between the first and 31-th modes are the vibration modes of cables. The vibration frequency of longer cable (from No. 27 to 34) are all less than 1.0 Hz. The vibration modes between the two fundamental modes of deck are caused by the interaction among these cables. A similar situation can be observed between higher modes of deck.

Table 1: The first five modal frequencies of the bridge deck (from FE model)

1st mode (1st mode)	2nd mode (31th mode)	3rd mode (64th mode)	4th mode (97th mode)	5th mode (102th mode)	6th mode (115th mode)	7th mode
0.515 Hz	1.051 Hz	1.446 Hz	1.757 Hz	1.894 Hz	2.038 Hz	2.224 Hz

3.2 Estimated dynamic properties of bridge deck from ambient data

Since most of the interesting dynamic responses of the bridge was associated with motions of the deck, then the vertical ambient vibration signals of the deck were collected. Fig. 5 shows part of the recorded signals (velocity) along the deck in the vertical direction. The signals collected at channels U1 and U5 were much smaller than the other channels because these channel locations were close to the pylon and at both ends of the bridge (close to the abutments). For each individual position, Fourier spectra were calculated. Fig. 6 only shows the Fourier amplitude spectrum of the vertical deck vibration at Channels U3 and U4. It is observed that for frequencies below 2.0Hz, there are several peaks in Fourier amplitude identified which are in consistent with the analytical results (as shown in Table 1). Based on the correlation AR model (as described in section 2.3) the system modal frequencies and damping ratios are identified, as shown in Table 3. A total of 70 orders in AR model was used in the analysis of the data. The identified first modal damping ratio of the deck (from channel U3 and U7 where significant vibration signals were observed) is between 1.1% ~3.5%. The damping ratio for frequency at 0.98Hz is about 0.6% or less. Vibration frequencies and damping ratios

estimation from cable vibration measurement were also processed in the same way. Data collected from cable and deck vibration simultaneously were analyzed. Fig. 7 shows the location of velocity sensors on one side of the cables and the deck. The vibration signal from channel U8 is also shown in the figure. The identified vibration frequencies from both channels U7 and U8 are shown in Table 4. It is observed that the first two identified vibration frequencies are consistent with the vibration frequencies of the bridge deck. The third vibration frequency is the first dominant frequency of the cable U8 which is consistent with the forced vibration frequency of the cable (see Table 2). Comparison on the Fourier amplitude spectrum between the recorded vertical responses of channels U7 and U8 indicate that the frequency interaction between deck and cable is obvious.

The vertical mode shapes of the bridge deck are also calculated from the ambient measurement. Two different approaches are implemented. First, the peak Fourier amplitudes and corresponding phase differences between different locations are used to extract mode shapes, as shown in Fig. 9. Second, based on the stochastic subspace identification technique, the mode shapes along the bridge deck are also estimated, as shown in Fig. 10. The estimated mode shapes of bridge deck are consistent with the results using a pick peaking method based on the Fourier amplitude spectrum. The first four identified deck vibration frequencies are also consistent. As for the vibration frequency of the fifth mode, both methods indicate different estimation value. Discussion on this inconsistency will be made as a comparison with the analytical result is conducted.

Table 2: The estimated cable vibration frequencies (Hz) of Gi-Lu cable-stayed bridge (from forced vibration test)

Ch-Chi Side (R33 &L33: Longest cable)

0.75823	R33	L33	0.75823
0.75513	R31	L31	0.75513
0.79146	R29	L29	0.79146
0.99956	R27	L27	0.99956
1.111	R25	L25	1.111
1.1161	R23	L23	1.1161
1.3042	R21	L21	1.3042
1.4196	R19	L19	1.4196
1.7411	R17	L17	1.7411
1.9493	R15	L15	1.9493
1.9581	R13	L13	1.9581
2.1138	R11	L11	2.1138
2.2756	R9	L9	2.2756
2.7106	R7	L7	2.7106
3.1737	R5	L5	3.1737
3.3889	R3	L3	3.3889
4.0191	R1	L1	4.0191

4.0193	R2	L2	4.0193
3.3891	R4	L4	3.3891
3.1738	R6	L6	3.1738
2.7108	R8	L8	2.7108
2.2758	R10	L10	2.2758
2.114	R12	L12	2.114
1.9582	R14	L14	1.9582
1.9493	R16	L16	1.9493
1.741	R18	L18	1.741
1.4193	R20	L20	1.4193
1.3037	R22	L22	1.3037
1.1149	R24	L24	1.1149
1.11	R26	L26	1.11
0.99808	R28	L28	0.99808
0.78728	R30	L30	0.78728
0.75068	R32	L32	0.75068
0.75464	R34	L34	0.75464

Lu-Ku Side (R34 & L34: Longest cable)

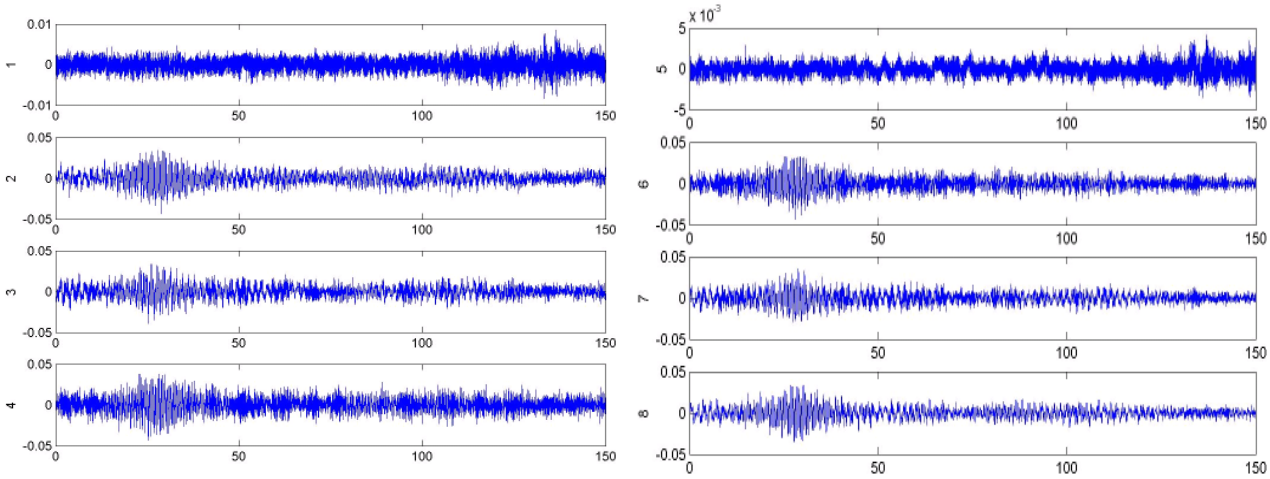

Fig. 5: Recorded ambient vibration signals (vertical direction) along the bridge deck.

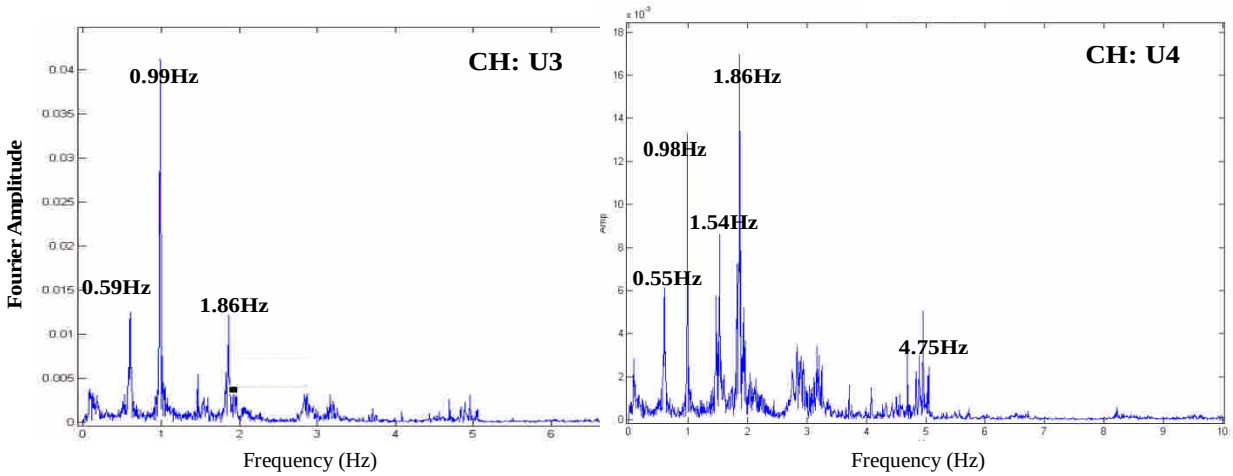

Fig. 6: Estimate Fourier amplitude spectrum of vertical ambient signal from Channels U3 and U4.

Table 3: identified modal frequencies and damping ratios form each observation channel using correlation AR model. Bold numbers indicate good correlation with the Fourier amplitude spectrum shown in Fig. 6.

	U1 (Deck-120L)		U2 (Deck-90L)		U3 (Deck-60L)		U4 (Deck-30L)		U5 (Deck-0)		U6 (Deck-30R)		U7 (Deck-60R)		U8 (Deck-90R)	
	f(Hz)	ξ	f(Hz)	ξ	f(Hz)	ξ	f(Hz)	ξ	f(Hz)	ξ	f(Hz)	ξ	f(Hz)	ξ	f(Hz)	ξ
1st	0.956	0.069	**0.586**	0.089	**0.593**	0.035	**0.554**	0.057	0.884	0.268	**0.562**	0.097	**0.601**	0.011	**0.599**	0.067
2nd	**1.429**	0.175	**0.986**	0.001	**0.986**	0.000	**0.981**	0.007	**1.462**	0.010	**0.984**	0.009	**0.986**	0.000	**0.986**	0.000
3rd	1.745	0.066	**1.602**	0.052	**1.801**	0.549	**1.536**	0.020	**1.900**	0.003	**1.561**	0.021	**1.684**	0.054	**1.561**	0.019
4th	2.876	0.019	**1.861**	0.001	**1.856**	0.001	**1.859**	0.001	2.910	0.007	**1.86**	0.001	**1.865**	0.003	**1.863**	0.001
5th	3.143	0.038	3.013	0.018	2.907	0.022	2.870	0.018	3.705	0.037	3.235	0.004	3.259	0.003	3.268	0.021
6th	4.550	0.001	3.950	0.040	3.334	0.081	3.194	0.018	4.397	0.021	3.57	0.046	3.715	0.006	3.308	0.202
7th	4.744	0.031	4.436	0.048	3.800	0.122	4.094	0.062	4.960	0.001	4.559	0.011	4.776	0.019	4.301	0.014
8th	6.007	0.003	**4.942**	0.006	**4.729**	0.012	**4.752**	0.010	5.536	0.031	**4.966**	0.002	**4.960**	0.002	**4.952**	0.002
9th	6.339	0.040	5.745	0.071	4.961	0.002	4.961	0.001	6.484	0.038	5.099	0.061	5.869	0.113	5.941	0.075
10th	7.211	0.003	6.630	0.019	6.209	0.036	5.752	0.045	7.446	0.003	5.929	0.141	6.594	0.545	6.755	0.015

Table 4: Identified modal frequencies (Hz) and damping ratios from Channels U7(deck) and U8(cable)

f (cable U8)	0.602	0.9841	**1.428**	2.396	2.825	3.274	4.267	4.905
ξ(cable U8)	0.0041	0.003	**0.001**	0.0048	0.0043	0.0036	-----	0.0048
f (deck U7)	0.602	0.984	1.659	1.898	2.419	3.286	4.812	4.917
ξ (deck U7)	0.0014	0.0001	0.0279	0.0027	-----	0.006	-----	0.0031

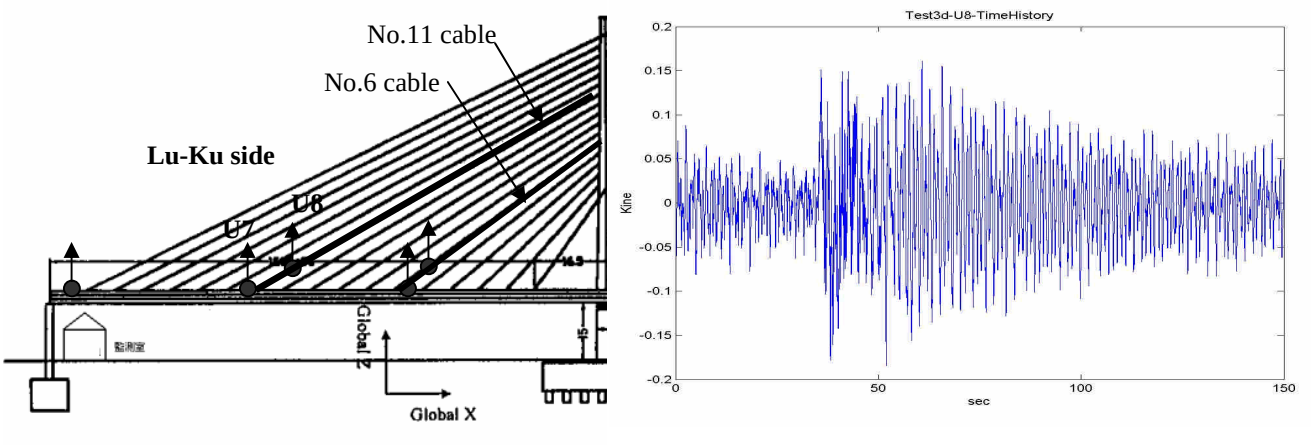

Fig.7: Test setup on Lu-Ku side to measure the ambient vibration signal of both deck and cables simultaneously. The recorded velocity on cable U8 is also shown.

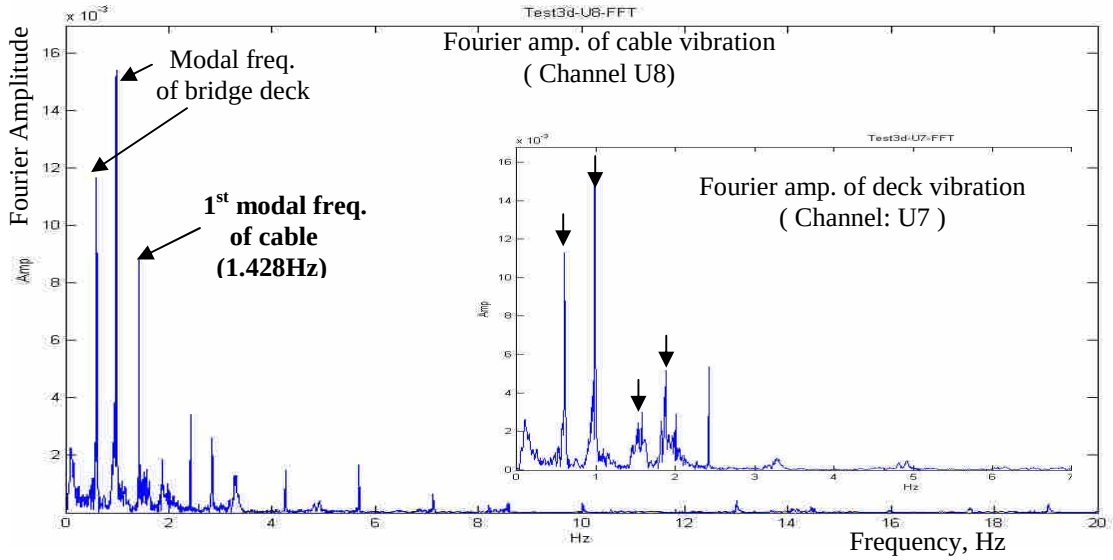

Fig. 8: Comparison on the Fourier amplitude spectrum from data of Channels U7 (deck) and U8 (cable).

3.3 Discussion between analytical and experimental results

As discuss in Section 3.1 the first seven vibration frequencies which represent the significant vibration modes of the bridge deck, was shown in Table 1. Fig. 11 plots the mode shapes of 1st, 31th, 64th, and 102th of the cable-stayed bridge from the analytical model. The shape along the deck from the analytical results is the same as the identified mode shape from ambient vibration data. The mode shapes along the bridge deck are consistent with the results from ambient vibration survey (from comparison among Fig. 9, Fig. 10 and Fig. 11). The identified modal frequency using different approach will induce little difference between them, particularly for the higher frequency mode.

4 CONCLUSIONS

The purpose of this paper is to conduct the ambient vibration survey of a cable-stayed bridge and develop a systematic method to extract the dynamic characteristics from ambient vibration data collected by a novel wireless monitoring system. The following conclusions are drawn from the full-scale measurements made on the bridge:

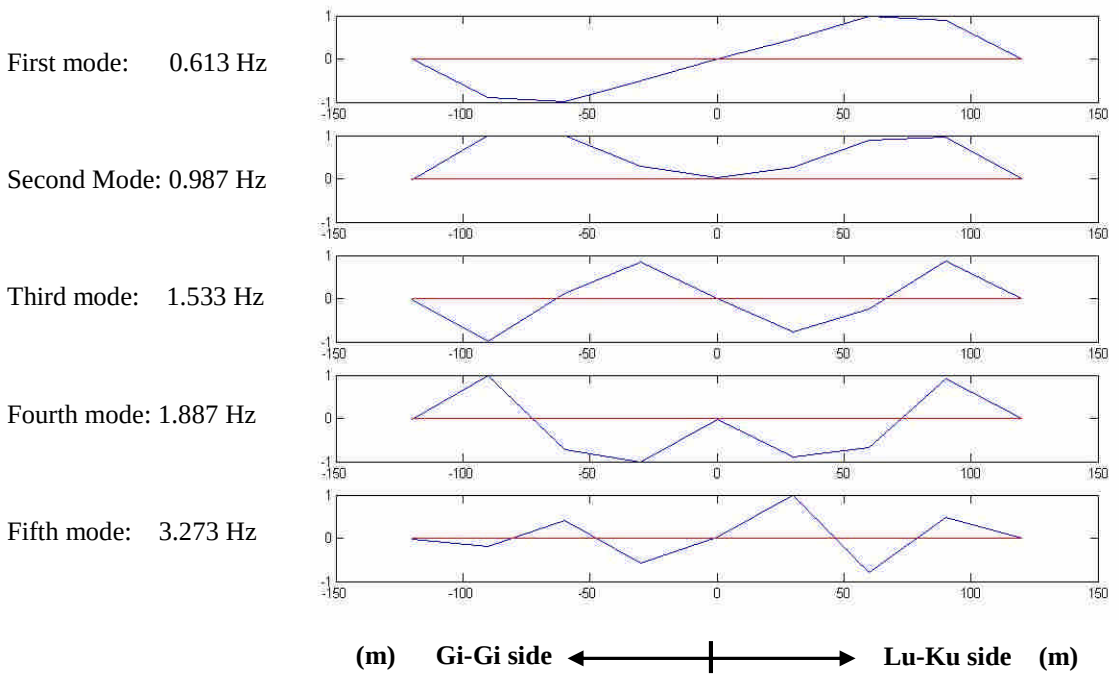

Fig.9: Identified the five vertical mode shapes of the bridge deck using Fourier amplitude and phase spectrum of vertical vibration signals collected along the bridge deck..

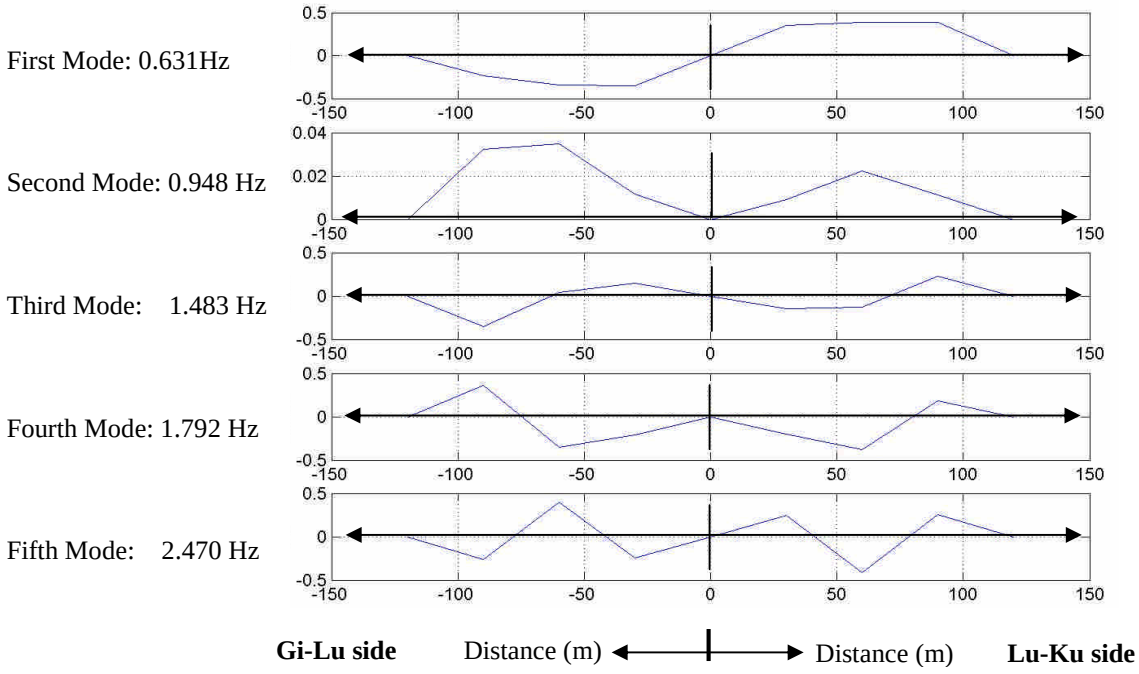

Fig. 10: Identified first five modes from ambient vibration measurement of Gi-Lu cable stayed bridge (in vertical direction of the bridge deck)

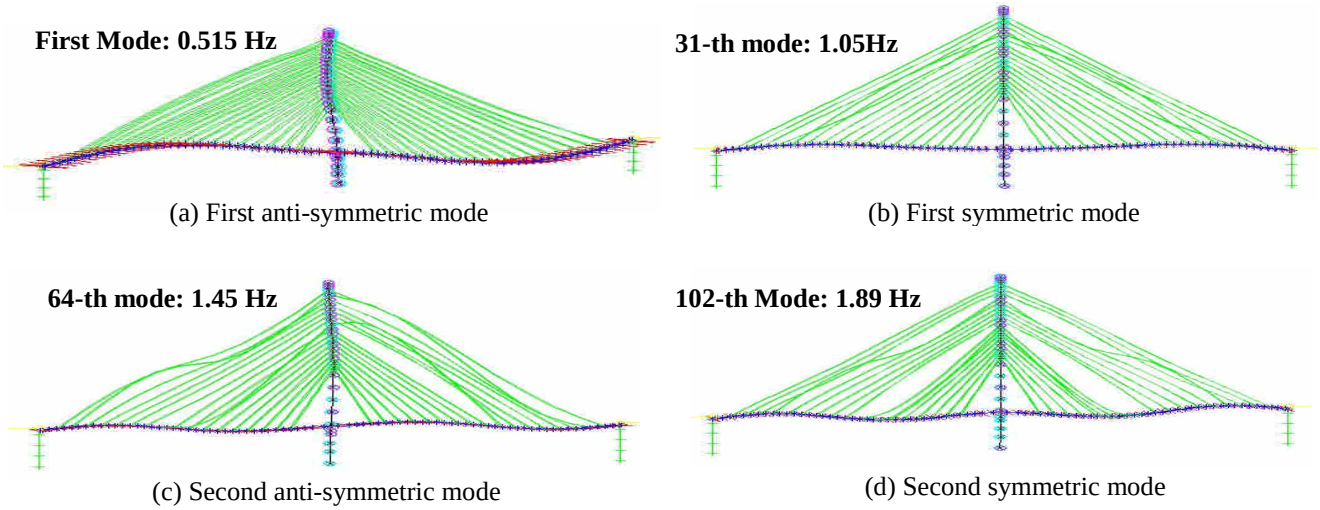

(a) First anti-symmetric mode

(b) First symmetric mode

(c) Second anti-symmetric mode

(d) Second symmetric mode

Fig. 11: Calculated mode shapes which are related to the deck vibration modes using analytical finite element model.

1. The wireless sensing units were used instead of using the traditional cable sensors. Less effort and man-power were required during the measurements. Because of the wireless communication length in open field can reach to 400 meters then it is possible to collect at least 12 sensors simultaneously with sampling rate of 100 points per second.
2. The measurement of structural response to ambient levels of winds and traffic induced vibrations has proved to be an effective means of identification of the dynamic properties of full-scale cable-stayed bridge. The dynamic properties that have been identified from these measured responses are modal frequencies, mode shapes and estimates of modal damping ratios.
3. To extract the dynamic characteristics from the response measurements, two different approaches were used: one was using the auto-correlation AR model applied to each set of data from the multiple channels and the other was the stochastic substructure identification method. The auto-correlation method can only estimate the modal frequencies and damping ratios directly from each measured response. To avoid the noise effect, the AR-model order is set to 70. Mode shapes can also be estimated by using the Fourier amplitude spectrum and the phase spectrum. As for the identification of mode shapes, the stochastic substructure identification can extract the system state matrix and then solve for eigenvectors (mode shapes). There are many approaches to deal with the spatial data and to extract eh mode shapes of the vibration structure, such as the Frequency domain decomposition method (FDD) [12]. More detail study is necessary in this direction.
4. The results of this test have provided conclusive evidence of the complex dynamic behavior of the bridge. The dynamic response of the cable-stayed bridge is characterized by the presence of many closely spaced, coupled modes. Significant experimental evidence was found to suggest that vertical vibration of the bridge deck is coupled with cable vibration within the frequency range of 0-3 Hz. This coupling effect was also observed from the study of the analytical finite element model. Since there is no measurement in the transverse direction in this study, then the coupling effect between the vertical-transverse-torsion deck response and the cables can not be examined. But from the analytical analysis, this coupling effect is also significant for the cable-stayed bridge.
5. The stochastic subspace identification provides a very effective way to identify the mode shapes of the structure through the spatially distributed sensors. As for the damping ratio estimation the first vibration mode of deck was between 3.5% ~9.5% (depends the estimation from different location). More detail study on the estimation of accurate damping ratios is needed in the future research.

5 ACKNOWLEGEMENTS

The authors wish to express their thanks to Central Weather Bureau (MOTC-CWB-94-E-13) as well as National Science Council (NSC94-2211-E-002-049) on the support of this research. The finite element mode shapes in Fig. 8 was prepared by Mr. Chia-Ming Chang and is referenced in companion papers.

REFERENCES

1. Ko, J.M., Sun, Z.G. and Ni, Y.Q., "Multi-stage identification scheme for detecting damage in cable-stayed Kap Shui Mun Bridge", Engineering Structures, Vol. 24, No. 7, 857-868, 2002.
2. Ozkan, E., Main, J. and Jones, N.P., "Long-term Measurements on A Cable-stayed Bridge," IMAC-paper, 2001.
3. He, X. et al., "System identification of New Carquinez bridge using ambient vibration data," Proc. Of Int. Conf. on Experimental Vibration analysis of Civil Engineering Structures, France, 26-28, Oct., 2005
4. Wenzel, H. and Pichler, D. Ambient Vibration Monitoring, John Wiley & Sons, Ltd, 2005
5. Straser, E.G. and Kiremidjian, A.S.,"A modular, wireless damage monitoring system for structure," Report No.128, John A. Blume Earthquake Center, CE Department, Stanford University, Stanford CA., 1998.
6. Lynch, J.P., Sundararajan, A., Law, K.H., Kiremidjian, A.S., and Carryer, E., "Power-efficient data management for a wireless structural monitoring system," Proceedings of the 4th Int. Workshop for SHM, Stanford University, Stanford, CA. (2003a).
7. Lynch, J.P., Sundararajan, A., Law, K.H., Kiremidjian, A.S., Kenny, T.W. and Carryer, E., "Embedment of structural monitoring algorithms in a wireless sensing unit," Structural Engineering and Mechanics, Techno Press, 15(3): 285-297 (2003b).
8. Lynch, J.P., Law, K.H., Straser, E.G., Kiremidjian, A.S., and Kenny, T.W., "The Development of a Wireless Modular Health Monitoring System for Civil Structures,", Proc. Of the MCEER Mitigation of Earthq. Disaster by Advanced Tech. (MEDAT-2) Workshop, Las Vegas, NV, Nov. 30, 2000.
9. Safak, E., "Identification of linear structures using discrete-time filters," ASCE, J. of Structural Engineering, Vol.117, No.10, 3064-3080, 1991.
10. Bart Peeters and Guido de Roeck, "Reference-based stochastic subspace identification for output-only modal analysis," Mechanical system and Signal Processing, 13(6), 855-878,1999.
11. Loh, C. H. & C. M. Chang, "MATLAB-based Seismic Response Control of Cable-Stayed Bridge : Considering Cable Vibration," J. of Structural Control & Health Monitoring (accepted for publication), 2005
12. Brincker, Rune, L.Zhang and P. Anderson, "Model identification of output-only systems using frequency domain decomposition," Smart Material & Structures, 10, 441-445, 2001.